Study of atmospheric dispersion under low wind speed conditions

P. Boyer,[a] O. Masson,[a] B. Carissimo,[b] F. Anselmet[c]
[a]*Institut de Protection et de Sûreté Nucléaire, Département de Protection de l'Environnement et des Installations, SERE, bât. 153, 13108 St Paul Lez Durance Cedex, France*
[b]*EDF/DER/DEAA, 6 Quai Watier, 78401 Châtou Cedex, France*
[c]*IRPHE/IMST, 12 Avenue Général Leclerc, 13003 Marseille, France*

Abstract

This paper presents the analysis of atmospheric SF_6 tracing experiments carried out under low wind speed conditions associated with strong thermal stability on a flat terrain. Analysis of meteorological data, processed in the form of probability densities, reveals that unsteady character of the current increase the greater the stability. The spectral densities of the three wind components deduced from sonic anemometers show that the horizontal current is dominated by large-scale turbulent structures, and that there is a weakening of energy levels in the neighborhood of 0,01 Hz. Tracings confirm that the levels of ATC (Atmospheric Transfer Coefficient) are greater the stronger the stability. Release impact is as closely linked to the increase in pollutant residence time as to higher instantaneous concentration levels. Lastly, ATCs deduced from a gaussian model being developed at IPSN gives good agreements with the experimental values.

1 Introduction

Dispersion process modeling in low wind speed conditions (U < 2 m/s) is still one of the most difficult. This kind of situation is typified by important spatio-temporal variations in the direction of wind and by important pollutant residence times at ground level up to several kilometers from the source. When these conditions are coupled with a temperature inversion (strong atmospheric stability), mechanical turbulent production is nil (Kristensen [1]) and the thermal turbulent production becomes negative. Current is dominated by important turbulent structures which make the notion of average direction and average wind speed far less realistic. In the absence of a channeling effect due to land contours, these structures create more or less important plume undulations. At this moment the polluted sector is important and abnormally high concentration levels may remain locally in the course of time (Crabol [2]).

From the point of view of efficiency of the dispersion process, these conditions are therefore the most penalizing. Classic models based on the hypotheses of homogeneous field are no longer valid. Modeling such a process still lacks theoretical bases (Anfossi [3]). The study of the phenomenon needs experiments enabling one to understand atmospheric turbulence and the unsteady and variable nature of the current.

2 Presentation of the dispersion experiments

IPSN and EDF have joined together to carry out three SF_6 tracing dispersion experiments in low wind speed situations, coupled with thermal stability on the site of the Salon de Provence airfield. The experiments (named S8, S9 and S10) were realized by night in the presence of temperature inversion and an average wind speed at ground level of less than 2m/s. The site is 2,5 km long and 2 km wide (figure 1). It is located on a plain surrounded by two small hills. The first rises to 250 m, three kilometers to the north-east, and the second to 150 m, two kilometers to the south-east of the site. All the western part opens towards the vast plain of La Crau. Towards the south is the Etang de Berre (lake) 3 km away, and the Mediterranean sea at 30 km. The lie of the land is perfectly flat and the roughness length is estimated at 0,05 m (Monin [4], Sutton [5]).

2.1 Atmospheric tracing method

The tracing device is made up of a system of SF_6 emission and about 40 gas sample automatic reading devices. The samplers are arranged under the wind of the emission point on three concentric cross-sections A, B and C located at 500, 1000 and 1500 m from the emission point, with an angle opening of 120° (figure 1). For each experiment, 11 kg of SF_6 are emitted at constant flow for 30 minutes, 2m from ground level. From the beginning of release, all the samplers are activated. The continuous air samples are taken 1m from ground level by a periodical sampling every 15 minutes and over a total length of time of 5 hours. SF_6 amounts in air samples thus taken are determined later in laboratory by electron capture gas chromatography.

2.2 Meteorological instrumentation

The meteorological apparatus is mainly composed of four 3-D and high sampling frequency (21 Hz) sonic anemometers. Three of them are installed on a meteorological mast, located on the south-west of the site (point A) at levels 30, 11 and 6 m. The fourth is placed at point B, 3 m above the ground level. At the foot of the meteorological mast there is also a sodar. Thanks to this data and those from the sonic anemometer the average vertical wind profile between the ground level and 400 m may be obtained. Three classic meteorological stations are also located at points A, C and D.

3 Meteorological data analysis (figure 2)

These profiles show that there exist a considerable wind shear at 30 m altitude. All experiments show a wind rotation in the vertical direction unlike the theory

of Ekman's spiral. It seems that the altitude current is dominated by a phenomenon of land breeze and sea breeze system linked to the Mediterranean sea and by an effect due to the north relief at several kilometers from the site. Although the notion of average value is not compatible with the situations studied, it is necessary to determine several average parameters to characterize them (see Table 1).

Table 1. Main average parameters

	S 8	S 9	S 10
Date	17/08/93	19/08/93	22/08/93
Hour (UT)	23h45 - 04h30	01h15-06h15	22h45 - 03h45
Average speed	1,2 m/s	1,2 m/s	0,7 m/s
Average direction	40°	75°	145°
Thermal gradient	0,12 °C/m	0,20 °C/m	0,20 °C/m
Richardson number	0,24	1,65	1,73

Temperature gradient is estimated from average temperatures read on the 30 meters height of the meteorological mast, and is attributed to 1 m. Referring to the conditions researched, the values confirm that the experiments are all associated with a strong thermal inversion. The gradient Richardson number is the one relating to the Sonic 3, situated 6 m on the meteorological mast. This parameter is meaningful in the vicinity of the ground where the vertical temperature and speed gradients are large. The experiment took place in non-saturating humidity conditions so this term enables one to find down the assessment of atmospheric stability, on the basis of the following formula :

$$R_i = \frac{g}{T} \frac{\partial T / \partial z}{(\partial U / \partial z)^2} \qquad (1)$$

g = gravitational acceleration (m/s^2); T = temperature (K); U = speed (m/s) z = altitude (m). ***(Ri < 0: unstable; Ri = 0 : neutral; Ri > 0 : stable)***

3.1 Probability densities (figure 3)

For all the sensors, wind measurements during S8 show an homogeneous spread and well-centered around the average figure. Compared to S8, S9 experiment shows a better homogeneity of direction in the vertical plane than in the horizontal one. S10 experiment is subject to considerable fluctuations, whether in the horizontal plane, vertical plane or over a period of time. For all the experiments, the speed has never exceeded 3 m/s and the speed fluctuation ranges observed and the differences in direction were larger the more thermally stable the situation.

3.2 Spectral densities of wind components and isotropy analysis

Spectral densities of the three wind components are calculated from high frequency data supplied by sonic anemometers. Considering the low wind speeds studied and the measurement volume of the anemometer, cutoff

frequency for all the experiments is about 1 Hz. The spectral analysis of turbulence allows representation of the energy contribution of different turbulent structures from 10^{-4} to 1 Hz (see figure 4). The first observation is the predominance of low frequency contributions to the variances of horizontal speed components. This property which does not apply to the vertical component indicates clearly that the horizontal current is dominated by large size structures. Because of the strong stability, the vertical movements are annihilated. It is not surprising therefore to observe much lower energy levels for the vertical component than those for the horizontal components. So that, vertical diffusion will be less efficient than horizontal one. For the three experiments, the two horizontal components show an energy reduction in the neighborhood of 0,01 Hz that corresponds to a duration of about 1,5 minute. The cutoff between the average field and the turbulent field could be envisaged at this level. This result supports the reasoning of D.Anfossi [6], who specified an assessment of the speed and average direction of the wind every two or three minutes, for the modeling of the dispersion process in situations of low wind speed.

Figure 5 shows a representation of the spectral density nS(n) vs. frequency (n). The theory of Kolmogorov specifies that in the inertial zone the spectral densities evolve according to a -2/3 power law of the frequency, and that in this zone, there exists a 3/4 ratio between the spectral densities of the longitudinal component and the spectral densities of the two others components. This 3/4 ratio reflects the isotropy of the turbulent movements in the swirling structures typified by the frequencies of the inertial zone.

Consistency of nS(n) with the -2/3 energy law is ratified from 0,2 Hz for the horizontal components, and seems to hardly start at 1 Hz for the vertical component. This means that, in present conditions, the sonic anemometers barely allow one to reach the lower limit of inertial range frequency. Nevertheless, comparison with reference data given by Kaimal [7] similarly suggests, just as the study on isotropy shown below, that the inertial regime is not in our case affected by the importance of large scale movements. For all the experiments, the ratio between the spectral densities of the longitudinal component and those of the lateral one is in the neighborhood of 3/4 from 0,2 Hz. This result confirms that the inertial zone begins at 0,2 Hz for the two horizontal components. For the vertical one and in the range of frequencies analyzed, one cannot obtain an isotropic frequential field between the horizontal plane and the vertical direction, even if the general tendency towards 1 Hz comes considerably nearer. Above 1 Hz the figures increase abruptly du to the cutoff frequency of the sensor.

4 Tracing results and comparison with a gaussian model

The main parameter studied is the distribution of Atmospheric Transfer Coefficient (ATC) versus the azimuth for the three radial cross-sections. In health physics the ATC is directly proportionate to the exposure doses and it allows an impact assessment. It is expressed in the following way :

$$CTA = \frac{\int_{t=0}^{\infty} C(t) \cdot dt}{\int_{\text{start emission}}^{\text{end emission}} q(t) \cdot dt} \qquad (2)$$

t = time (s); C(t) = instantaneous concentration (kg/m³); q(t) = emission rate (kg/s)

On the cross-section at 500 m, comparison between the three experiments (figure 6) shows that the ATCs are equivalent for S8 and S9, and five times higher for S10. However, the differences between the experiments decrease as the distance from the source increases. This behavior confirms that near the source ATC levels are higher the stronger the stability. Figure 7 presents the time dependent evolution of average concentrations observed on each sampling cross-section. Comparison between experiments shows that maximal concentrations are globally the same. On the other hand, pollutant residence times show more significant differences. Differences in levels of ATCs observed between the three experiments are as linked to differences of pollutant residence times as to differences between concentration levels.

4.1 Comparison with a Gaussian model

A model being developed at IPSN was used in this frame. It is a gaussian puff model which takes into account an analytical solution of the diffusion equation.

$$\bar{C}(x,y,z,t) = \frac{Q_0}{(2\cdot\pi)^{\frac{3}{2}}} \cdot \exp\left[-\frac{1}{2}\cdot\left[\frac{(x-\bar{U}\cdot t)^2}{\sigma_x^2} + \frac{y^2}{\sigma_y^2} + \frac{(z-H)^2}{\sigma_z^2}\right]\right] \qquad (3)$$

The basic hypotheses are (a) transverse and vertical average speeds are nil, (b) the current is uniform over the height (constant speed) and (c) the turbulence is homogeneous. Up till now, IPSN has used for this type of model the practical standard deviations referred to as Doury's [8]. Development in progress (Romeo [9]) offers a more theoretical and physical approach with diffusion standard deviations calculated from the breakdown in frequency of turbulent energy. The model takes into account the speed and the average direction of wind, the level of atmospheric stability, the type of roughness, the flow duration and height of release. Table 2 gives the different calculation parameters used.

Table 2. Calculation parameters

	S 8			S 9			S 10		
	500m	1000m	1500m	500m	1000m	1500m	500m	1000m	1500m
Direction °	37	39	38	76	76	74	146	144	149
Speed m/s	1,1	1,1	1,2	1,2	1,1	1	0,8	0,7	0,6
Diffusion	low			low			low		
Roughness	low			low			low		

The direction and average wind speed are calculated by Sonic 4 located in the middle of the site.Values are determined over the period relative to transfer time at a given distance, increased by the duration of emission (Slade [10]).

Considering those previous hypotheses and the observed conditions, this kind of model is in fact used beyond its field of validity. However, the analytical approach proposed by this kind of modeling offers the advantage of considerable simplicity of use and a necessary speed of calculation in the event of emergency. What is more, this technique has the benefit of several dozen years experience in the nuclear field. From now on, the objective is to identify experimentally the eventual weaknesses of the model so as to correct its implementation for wind situations studied in this paper.

4.1.1 Comparison of ATC (figure 6) On the cross-section at 500 m, two different behaviors are observed. The first concerns S8 and S9 experiments which are typified by a transfer velocity that exceeds 1 m/s. The ATCs deduced from the model are three times greater than the experimental ones, and the plume spread is underestimated by a factor 2. The second type concerns S10 where transfer velocity is less than 1 m/s. The ATCs are up to three to four times greater than the experimental values. On the other hand it is not possible to estimate the plume spread because only one side of this plume has been measured. For the cross-section at 1000 m, the ATCs are underestimated for all trials. The differences between the experimental values and the theoretical ones decreases. The estimation of plume spread is good. At 1500 m, except for S10, the model is fairly close to the observed values.

Model precision increases as the distance from the source increases and the stability decreases. In all cases, the expected values are in the same order than the observed ones. This agreement show the aptitude of this model to forecast the ATCs distribution.

4.1.2 Comparison of average concentration evolution on each cross-section (figure 7) For all the experiments and on each sampling cross-section, evolution comparison over average concentration times observed shows that the model overestimates the plume transfer velocity. Maximum concentration levels are correct for S8 and S9 and they are in all cases underestimated for S10. It appears that for S8 and S9, the model tends to overestimate concentration levels and underestimate the transfer duration. These two tendencies compensate each other partly, which gives a better assessment of the ATCs than for S10. For S10 the concentration levels and transfer times have been underestimated. These two tendencies act in the same way and lead to a not so good assessment of the ATCs.

5 Conclusion

The probability densities of speed and wind direction show that variables in the dynamic field are higher the lower the average wind speed and the stronger the stability. Consequently, the angular sector covered by the plume increases when stability rises up. Analysis of wind component spectral densities confirms

that the horizontal current is mainly influenced by large-sized swirling structures and that vertical movements are reduced du to the stability.

The turbulent structures of the current concerning the inertial zone have an isotropic behavior in the horizontal plane. On the other hand, between the horizontal plane and vertical direction, this property has not really been detected because of the filtering effect resulting from the size of the sensors. Tracing analyses show that the main consequence of a gaseous release for conditions studied will be the presence of a stronger ATC the stronger the stability. This increase in the ATCs is more the result of an increase in residence times than in concentration levels. In terms of impact, this behavior - which is associated with a slowing-down of the plume at ground level and wind meandering - could, from the point of view of individual doses in critical situations, lead to overshoot of regulatory thresholds. For low wind speed situations, ATCs forecast by the IPSN gaussian model being developed lead to a good estimation of the collective dose. In such situation, the different probabilistic and spectral analyses show that a specific treatment which takes explicitly into account the lateral transport du to meandering could allow to consider this phenomenon and to obtain better results. Moreover, the comparison between the experimental and theoretical transfer times indicate that the slower displacement speed of the plume at ground level has to be taken into consideration.

Bibliography

1. L. Kristensen, N.O. Jensen, E.L. Petersen : Lateral dispersion of pollutants in a very stable atmosphere - The effect of meandering, *Atmospheric Environment* Vol. 15, 1981 p 837-844.

2. B. Crabol, G. Deville-Cavelin : Assessment of the dispersion of fission products in the atmosphere following a reactor accident under meteorological conditions of low wind speed, IPSN/DPEI/SERE, SRP Report N°84/10, 1984.

3. D. Anfossi : EURASAP Newsletter N°11, 1990.

4. A.S. Monin : The atmospheric boundary layer, *Ann. Rev. Fluid Mech.* Vol. 2, 1970 p 225.

5. O.G. Sutton : Atmospheric turbulence, London: Methuen & Co. LTD, Second Edition, 1955.

6. D. Anfossi, G. Brusasca., G. Tinarelle : Simulation of atmospheric diffusion in low wind speed meandering conditions by a Monte Carlo dispersion model, *IL Nuovo Cimento* Vol. 13 C, 1990.

7. J.C. Kaimal, J.C. Wyngaard, Y. Izumi., O.R. Cote : Spectral characteristics of surface-layer turbulence, *Quart. J. R. Met. Soc.* Vol. 98, 1972, p 563-589.

8. A. Doury & all : Abaques d'évaluation directe des transferts atmosphériques d'effluents gazeux, CEA report DSN n°84, 03/1977.

9. E. Romeo : Contribution to the study of turbulent diffusion of a pollutant in the atmosphere, Thesis, Pierre et Marie CURIE University, Paris VI, 1994.

10. D.H. Slade : Meteorology and atomic energy, United States Atomic Energy Commission TID-24190, 1968.

FIGURE 1 : EXPERIMENTAL ARRANGEMENT AND ATC's DISTRIBUTION
TRIAL S 10

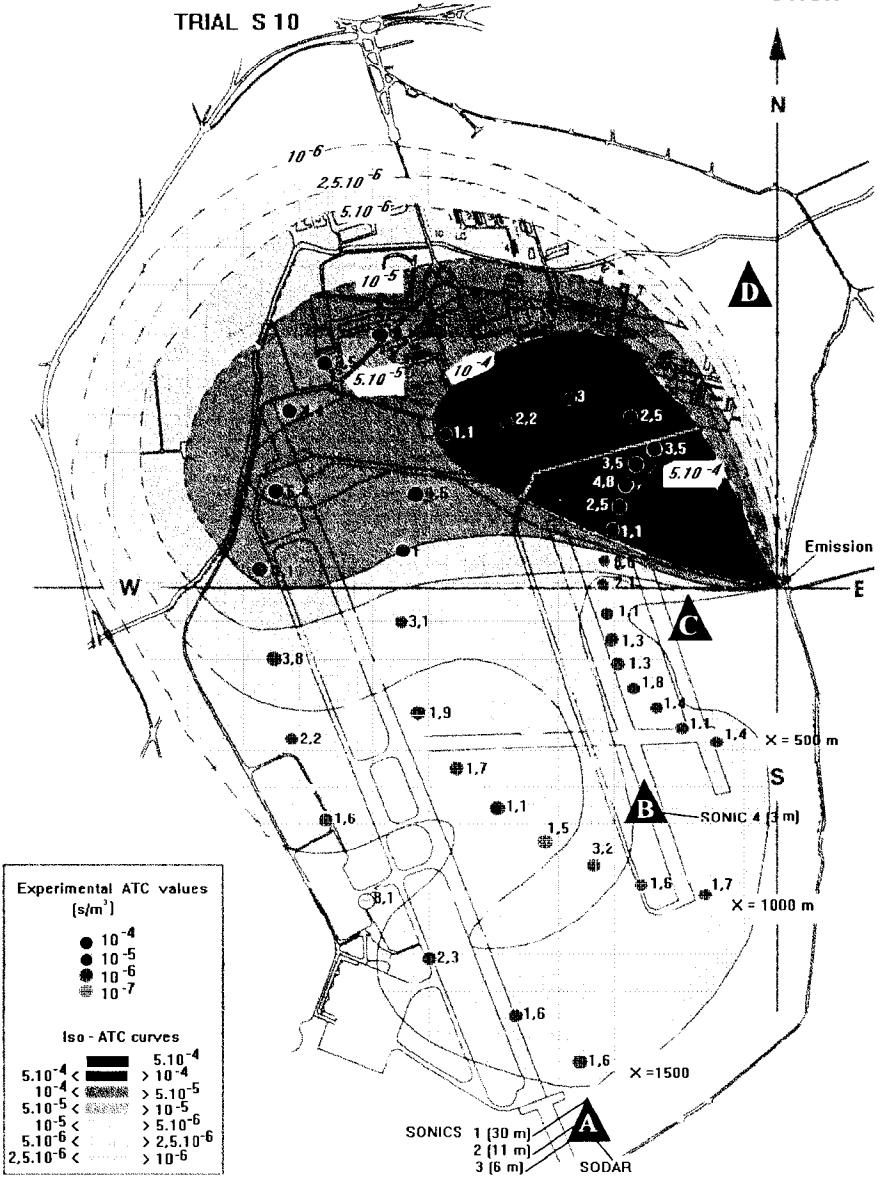

Figure 2 : Average vertical profiles of wind speed and direction

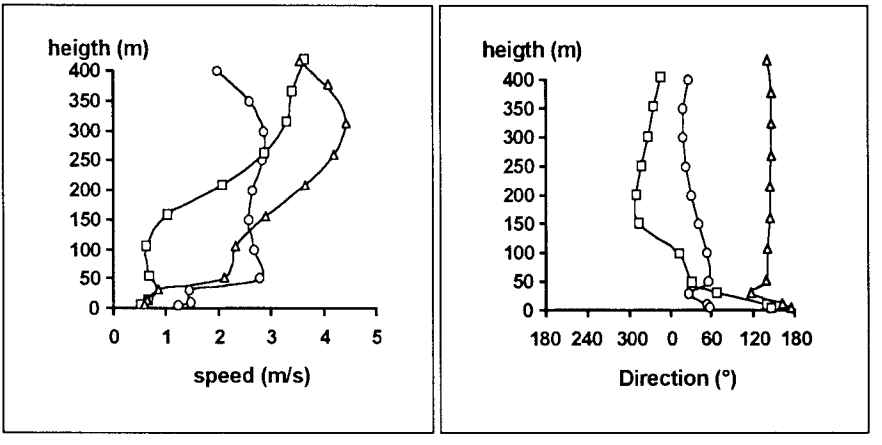

Figure 3 : Probability distribution of the wind direction

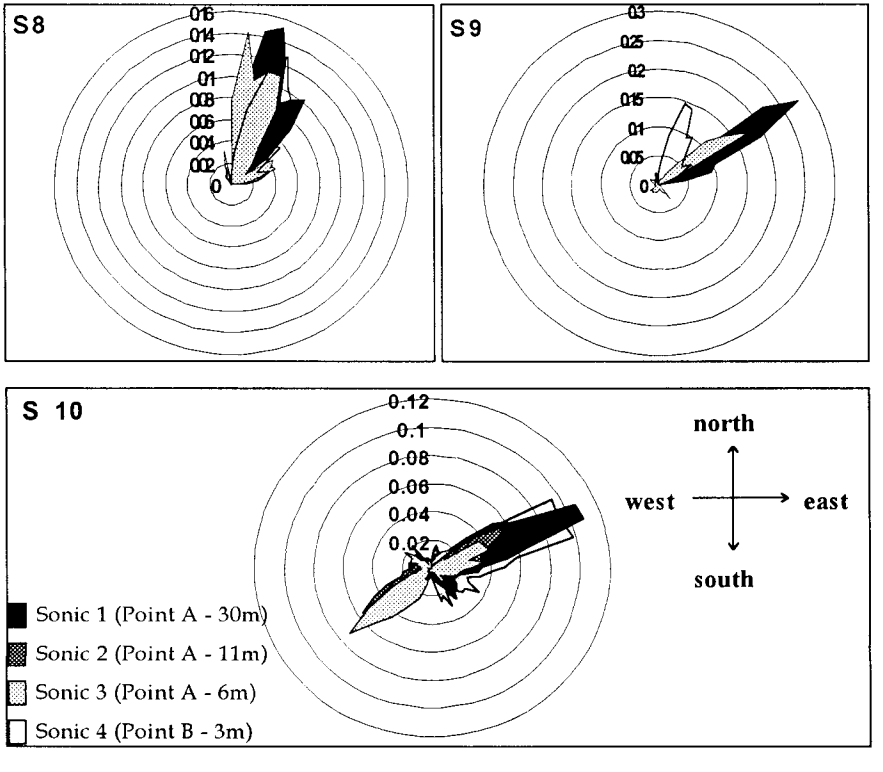

Figure 4 : Spectral densities of the wind components - Sonic 4

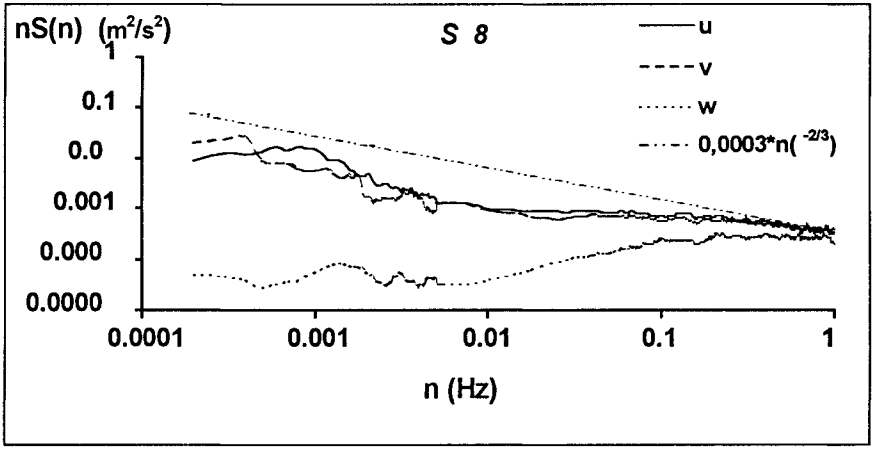

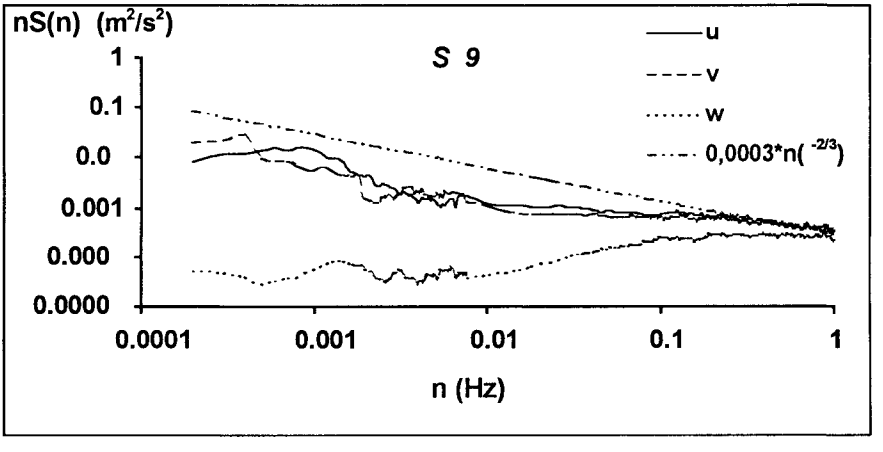

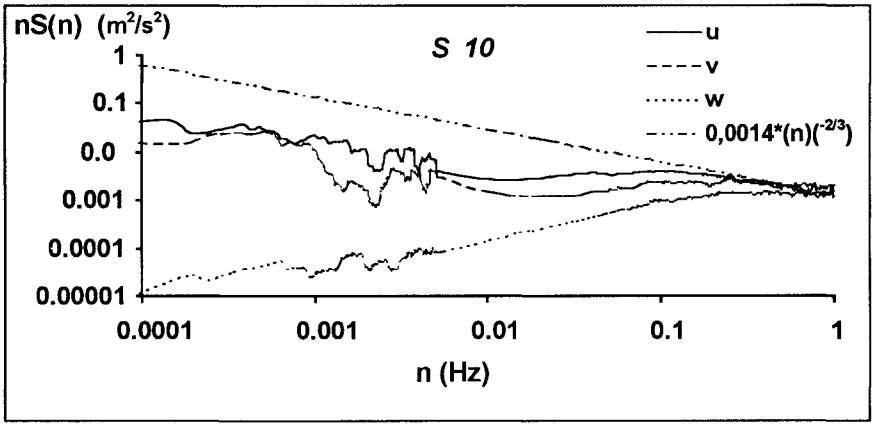

Figure 5 : Comparison between the spectral densities ratio and the 3/4 value

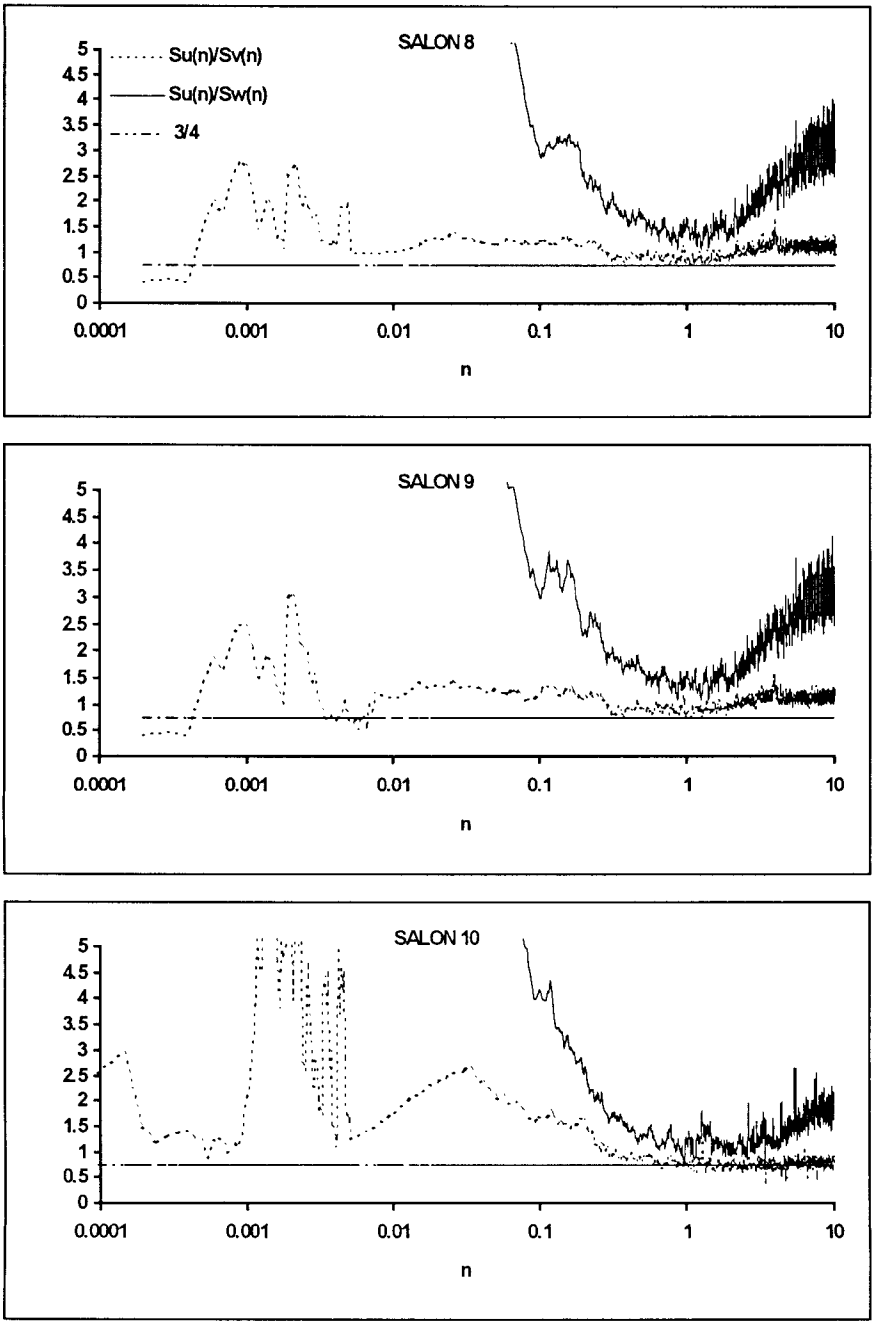

Figure 6 : Comparison between calculated and experimental ATCs distribution depending on the azimuth on each radial cross-sections

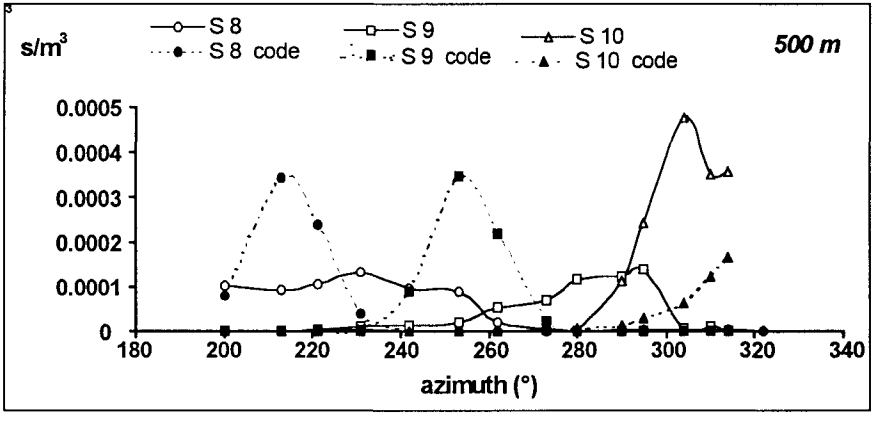

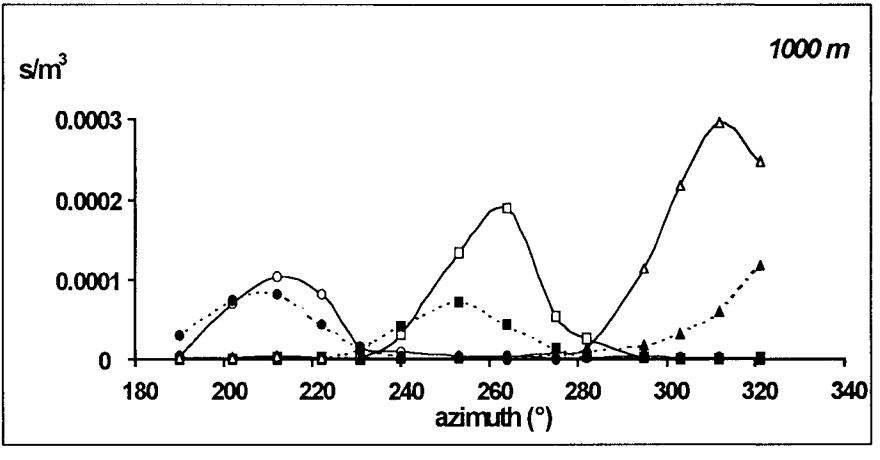

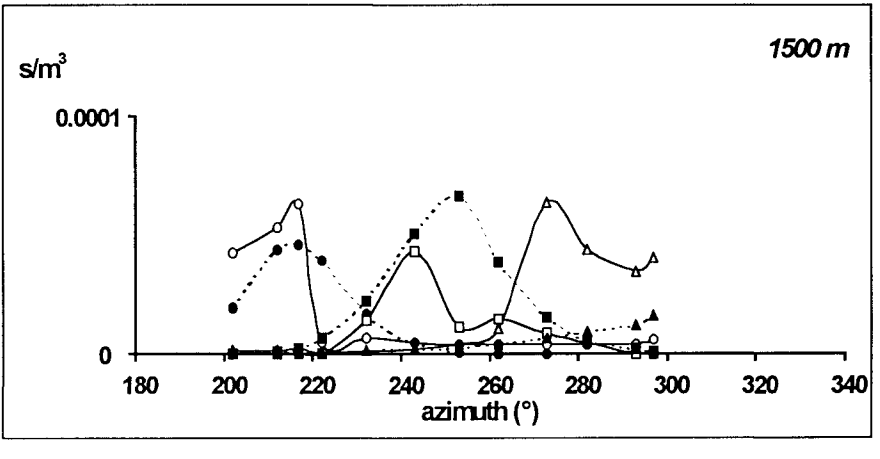

Figure 7 : Comparison between calculated and experimental evolutions of average concentrations on each cross-section vs. time